It's the Heat and the Humidity: The Complementary Roles of Temperature and Specific Humidity to Recent Changes in the Energy Content of the Near-Surface Atmosphere

P. C. Stoy,[1,2] J. Roh[1]

[1]Department of Biological Systems Engineering, University of Wisconsin – Madison

[2]Department of Atmospheric and Oceanic Sciences, University of Wisconsin – Madison

*pcstoy@wisc.edu

Corresponding author: Paul C. Stoy (pcstoy@wisc.edu)

Key Points:

- The temperature and specific humidity of the near-surface atmosphere are increasing.
- Both imply an increase in atmospheric energy content, and climate models often struggle to simulate regional changes.
- The rate of air temperature increase would have more than doubled without specific humidity change, all else being equal.

Abstract

Global change is a change in the planetary energy balance. It is usually expressed as a change in near-surface (2 m) air temperature (T_a), but changes to T_a represent only part of the atmospheric energy balance, which includes specific humidity (q) and more. We analyzed MERRA-2 reanalysis data and 15 Atmospheric Model Intercomparison Project (AMIP) models over the 1980-2014 period. Some 41%, 37%, and 49% of the near-surface atmosphere showed significant increases in E_T, E_{SH}, and E, respectively. The average increase in E_T (E_{SH}) was 10.6 J kg^{-1} year^{-1} (11.5 J kg^{-1} year^{-1}) but AMIP models estimated that E_T (14.5 J kg^{-1} year^{-1}) exceeded E_{SH} (13.7 J kg^{-1} year^{-1}). Global near-surface T_a would have increased at more than twice the observed rate if energy was not partitioned into latent heat. Results demonstrate the critical role that q plays in recent changes to near-surface atmospheric energy.

Plain Language Summary

Greenhouse gases trap energy, making it more difficult for energy to leave the planet. This has caused an increase in air temperatures near the surface, but there is much more to global change than air temperature alone. Most of the excess energy caused by the increase in greenhouse gases has entered the ocean, because it takes lots of energy to heat water. The water vapor content of the near the surface has also increased, and it takes energy to heat this water. We find that the energy needed to heat the extra water in the atmosphere has helped buffer increases in global air temperatures, which would have increased by more than double if energy was not needed to heat water in the air near the surface. Global climate models are able to simulate many aspects of these energy changes, but struggle in key regions where regional climate is complex. Many of the largest increases in atmospheric energy have occurred in most populous regions of the globe. It is important to understand that global change is a change in the energy balance of the planet, and that air temperatures alone are only a small (but important) part of this energy change.

1 Introduction

Global change is a change in the energy balance of the planet. It is usually communicated to the public as a change in near-surface (2 m) air temperatures (T_a), but some 90% of the excess energy has entered the oceans (Church et al., 2011; von Schuckmann et al., 2020) and T_a is only part of the energy balance of the near-surface atmosphere (Peterson et al., 2011). The total energy (E, J) of a parcel of air is the sum of its enthalpy, latent heat, kinetic energy, and gravitational potential:

$$E = mC_PT_a + mLq + \frac{1}{2}mv^2 + mgz \quad (1)$$

Where C_P is the specific heat of air (J kg^{-1} K^{-1}), T_a is in Kelvin, L is the latent heat of vaporization (J kg^{-1}), q has units of kg kg^{-1}, v is velocity (m s^{-1}), g is acceleration due to gravity (m s^{-2}), z is height (m), and we assume an air parcel mass (m) of 1 kg. The gravitational term is not changing and changes to the kinetic term is trivial compared to those of enthalpy and latent heat (Peterson et al., 2011) despite well-documented changes in global wind speed (McVicar et al., 2012).

Models anticipate that *relative* humidity should be largely unchanging (Byrne & O'Gorman, 2016; Dessler & Sherwood, 2009; Held & Soden, 2006; Schneider et al., 2010) but the observational record indicates a slight drying (Ficklin & Novick, 2017; Willett et al., 2020;

Willett et al., 2014), and even a constant relative humidity on a warming planet implies an increase in q and latent heat due to the Clausius-Clapyron relation. How do these changes in both T_a and q impact E and are models able to accurately simulate their recent changes?

It is valuable to communicate changes in the global energy balance using the correct physical variables (Pielke et al., 2004, 2007), but terms like ‘enthalpy’ and ‘latent heat’ are not in the common lexicon. It is more commonly understood that it takes a substantial amount of energy to heat water and it follows – if the atmosphere can hold more water as temperatures increase – that more energy is required to heat this extra water. Although these notions are arguably simple, communicating them remains a challenge and public perception of the magnitude of global energy changes may be underestimated as a consequence. Here, we study data from the Modern-Era Retrospective analysis for Research and Applications, Version 2 (MERRA-2) to quantify the importance of changes in both T_a and q to changes in E. We also study the ability of global models to simulate these changes with a focus on the period following the 1980 global temperature ‘regime shift’ (Reid et al., 2016). We focus our discussion on the importance of communicating the roles of both enthalpy and latent heat as critical parts of energy changes in the Earth system due to anthropogenic global change (Church et al., 2011; von Schuckmann et al., 2020).

2 Materials and Methods

We analyzed MERRA-2 (Gelaro et al., 2017) global gridded data products and 15 models from the Atmospheric Model Intercomparison Project (AMIP, Table 1) (Eyring et al., 2016) over the 1980-2014 period. The end of the study period was selected due to uniform data availability. For each pixel of the MERRA-2 and AMIP datasets, T_a was multiplied by C_P (1005 J K^{-1} kg^{-1}) to obtain enthalpy for a 1 kg parcel of air following Peterson et al. (2011), which we abbreviate E_T as 'energy content due to temperature'. q was multiplied by L (2.45 × 10^6 J kg^{-1}) to obtain latent heat as 'energy content due to specific humidity' (E_{SH}) (Equation 1), again for a 1 kg air parcel. E was taken to be the sum of E_T and E_{SH} following the assumptions discussed above.

The nonparametric Thiel-Sen estimator ('Sen's slope') was used to quantify significant trends in E_T, E_{SH}, E on a per-pixel basis using the 'trend' package (Pohlert, 2020) in R (R Core Team, 2020) for the MERRA-2 dataset. For the AMIP models, changes in E_T, E_{SH}, E were calculated after first averaging to a common spatial scale (Table 1). Trends were then calculated using Sen's slope and an average trend then was calculated for each pixel. We repeated the analysis by first averaging E_T, E_{SH}, E for all 15 models and then calculating slopes. Slopes with $P < 0.05$ were considered to be statistically significant.

We also calculated the T_a change that would result if all near-surface energy was partitioned to enthalpy rather than latent heat (Equation 1), all else being equal, including changes in circulation that would inevitably result from such changes in energy partitioning (Avissar, 1995). Results are subject to uncertainties in the MERRA-2 dataset and the observations and methods that it uses to create the reanalysis product over land and oceans (Bosilovich et al., 2017; Gelaro et al., 2017).

3 Results

Using MERRA-2 reanalysis data for the 1980-2014 period and interpreting significant changes using Sen's slope, 41% of near-surface atmosphere pixels experienced a significant increase in

E_T, 37% had a significant increase in E_{SH}, and 49% had a significant increase in E (Figure 1). The observed average increase in E_T (E_{SH}) was 10.6 J kg^{-1} year^{-1} (11.5 J kg^{-1} year^{-1}); changes in E_{SH} due to changes in q contributed 8.5% more to global E during the study period, on average.

Significant increases in E_T were observed across the globe, especially over land, and especially across high-latitude regions where it frequently exceeded 80 J kg^{-1} year^{-1} except for the Southern Ocean which was dominated by significant decreases in E_T (Figure 1A). Significant increases in E_{SH} greater than 80 J kg^{-1} year^{-1} were observed across parts of Central America, the Mediterranean and Middle East, South Asia, and the Maritime Continent. There were notable significant decreases in E_{SH} across parts of Africa and South America (Figure 1B). As a result, increases in E greater than 80 J kg^{-1} year^{-1} were widely distributed across the globe from tropical to polar zones (Figure 1C).

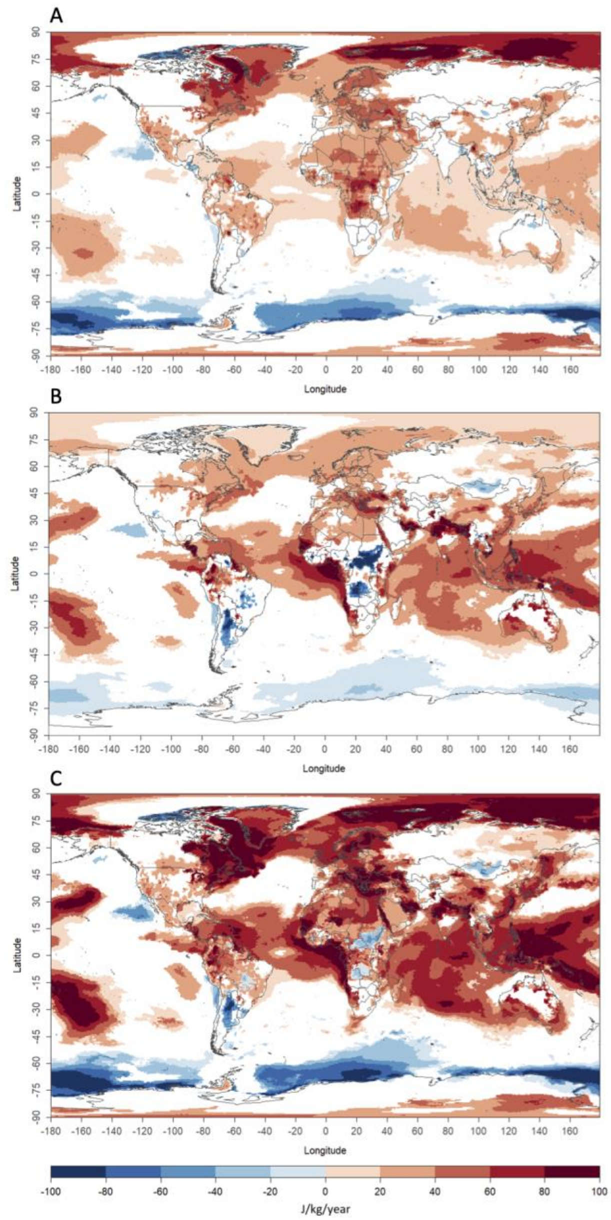

Figure 1: Observed trends in near-surface (A) enthalpy (E_T), (B) specific heat (E_{SH}), and (C) total energy (E) taken to be the sum of E_T and E_{SH} from 1980 to 2014 from MERRA-2. White pixels indicate insignificant trends ($P > 0.05$) calculated using Sen's slope.

AMIP models estimated an average E_T (E_{SH}) increase of 14.5 (13.7) J kg^{-1} year^{-1}. (Repeating the analysis by first averaging energy terms, then calculating slopes, resulted in an E_T (E_{SH}) increase of 17.4 (16.8) J kg^{-1} year^{-1}.) In other words, AMIP models tended to overestimate global near-surface *E* changes *versus* the MERRA-2 reanalysis and estimated that this change was caused more by changes in T_a than *q*. The AMIP models incorrectly simulated the spatial distribution of E_T changes across much of the Arctic and its magnitude across much of the Southern Ocean and Africa (Figure 2A). The AMIP models incorrectly simulated E_{SH} changes across much of Africa and other parts of the tropics and subtropics, on average (Figure 2B), such that changes in *E* across many regions of the globe differed between the MERRA-2 reanalysis and AMIP models (Figure 2C).

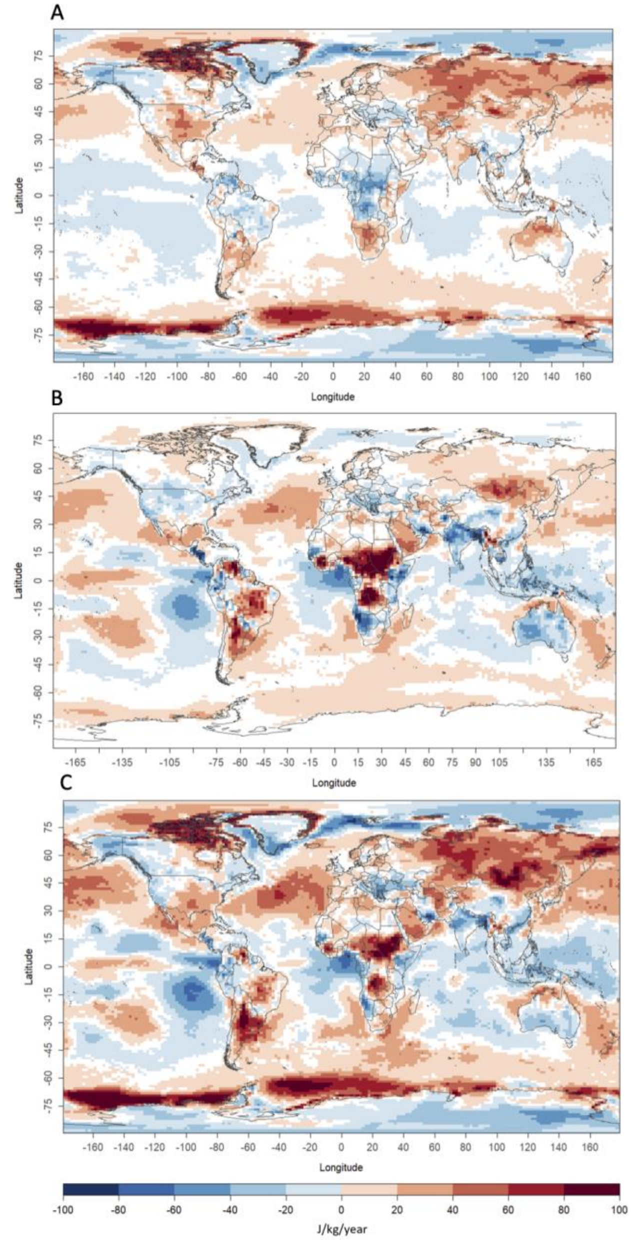

Figure 2: The difference between the mean of 15 AMIP models (Table 1) and MERRA-2 for trends in near-surface enthalpy (E_T, A), latent heat (E_{SH}, B), and enthalpy plus latent heat (E, C) from 1980 to 2014. Positive values indicate that the mean AMIP model is significantly greater than MERRA-2 trends. White pixels indicate insignificant trends ($P > 0.05$) calculated using Sen's slope.

Global T_a would have increased far more than observed across the study period (Fig. 3A) if all excess energy was partitioned into enthalpy (Fig. 3B), all else being equal. In this hypothetical scenario, many of the regions that would have experienced increases in T_a in excess of 2.4 °C over the 35-year study period are in subtropical and tropical regions with characteristically hot temperatures and large (or growing) populations including the Mediterranean, the Persian Gulf region, South Asia, and East Asia (Fig. 3B).

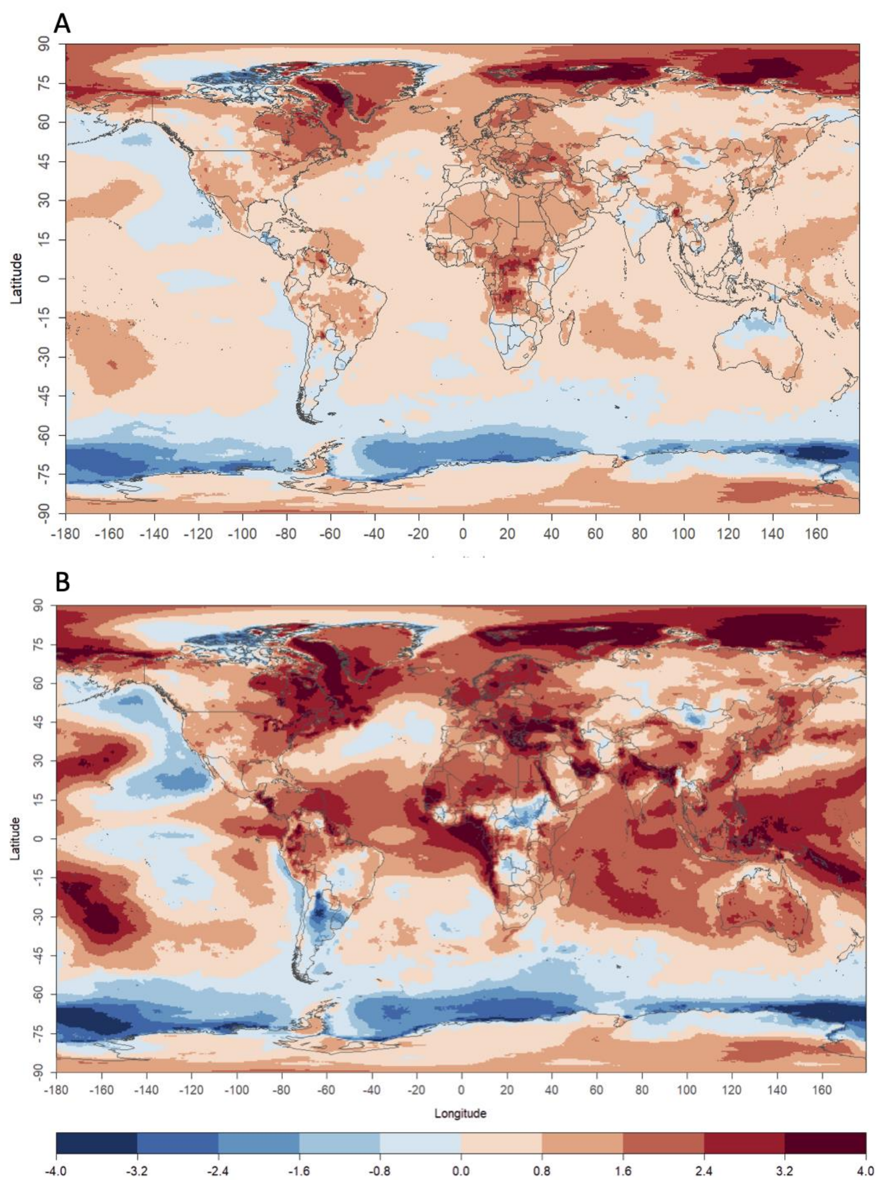

Figure 3: The observed change in (A) air temperature (°C / 35 years) for the 1980-2014 period from MERRA-2 and (B) the change in air temperature that would have resulted if the observed change in near-surface energy from MERRA-2 was partitioned entirely into enthalpy rather than latent heat, all else being equal.

4 Discussion

Results are similar to those reported by Peterson et al. (2011) for the 1973-2003 period using meteorological station data over land, who note that the energy content of the near-surface atmosphere increased at a rate of 29 J kg^{-1} $year^{-1}$. Our observed rate of 22 J kg^{-1} $year^{-1}$ is lower but includes oceans where T_a and E_T changes are less pronounced, where most excess energy due to anthropogenic global change is stored (Church et al., 2011; von Schuckmann et al., 2020), and whose temperatures continue to increase (Cheng et al., 2021). Peterson et al. (2011) note decreases in q across some areas of the subtropical Southern Hemisphere as also observed here (Figure 1B) that are largely not captured by AMIP models (Figure 2B), suggesting that the mechanisms underlying these changes in atmospheric moisture must be understood to accurately capture regional changes in atmospheric energy content. Notable of these include the transition zones between the Congo Rainforest and the Sahara and Kalahari Deserts whose climate is determined by a complex interaction between ocean dynamics (Held et al., 2005), the dynamics of the intertropical convergence zone, vegetation feedbacks (Zeng et al., 1999), and anthropogenic effects including aerosols (Held et al., 2005) with uncertain climate effects (Schwartz & Andreae, 1996), all of which remain a challenge for climate models. Likewise, models correctly predict arctic warming (Figure 2), but simulating the spatial patterns of this warming remains a challenge due in part to known challenges in modeling the remarkable rate of observed sea ice decline (Stroeve et al., 2007). Correctly modeling the Southern Ocean also remains a challenge due to the combined impacts of glacial melt (Rye et al., 2020), wind forcing, and greenhouse gas forcing (Kostov et al., 2018). In other words, regions where AMIP estimates of E and its terms poorly match MERRA-2 are those where model development is rapidly progressing.

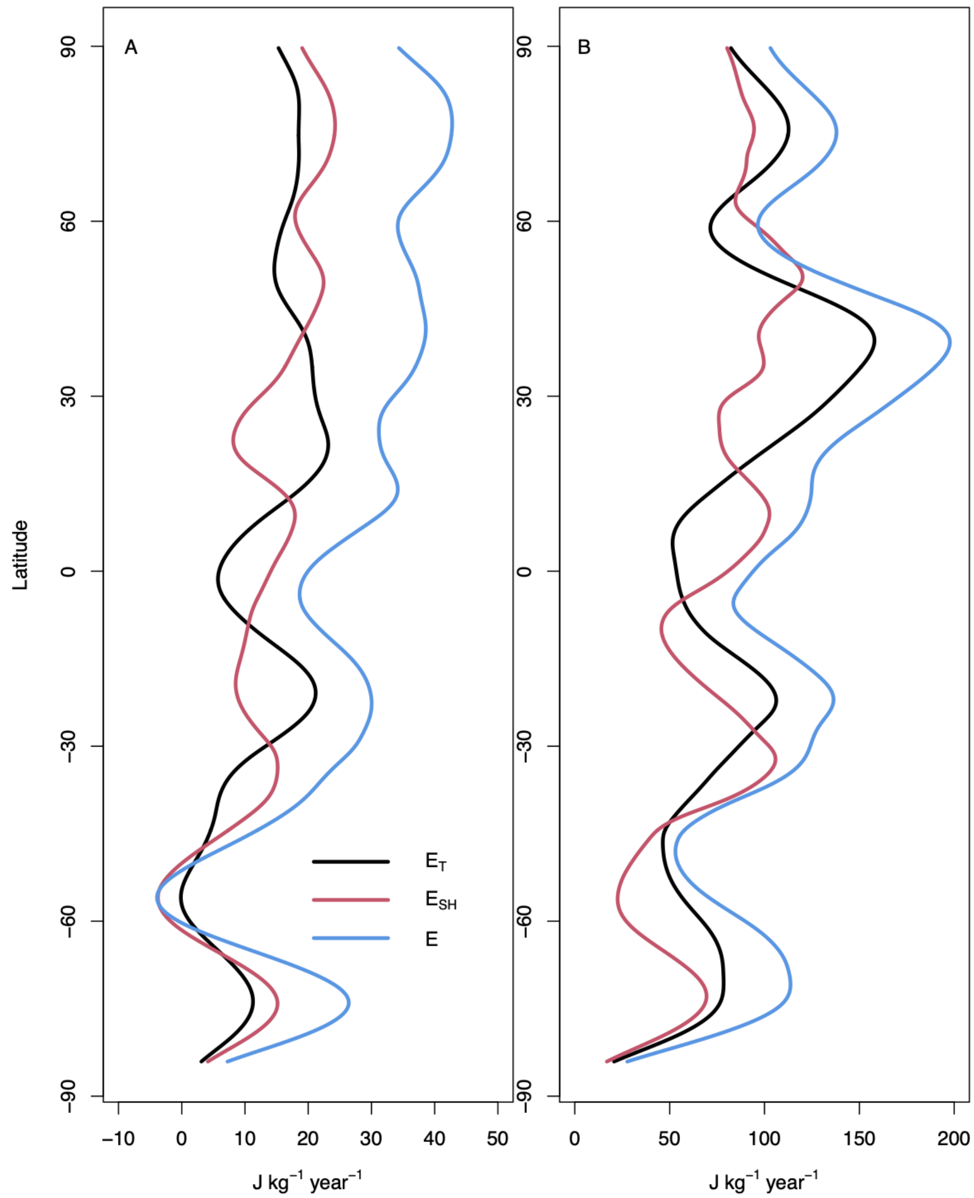

Figure 4: The average (A) and maximum (B) changes in trends in near-surface enthalpy (E_T), latent heat (E_{SH}), and enthalpy plus latent heat (E) from MERRA-2 for the 1980-2014 period as a function of latitude. Data were smoothed using a Butterworth filter using the 'signal' package in R (Ligges et al., 2013).

q and E_{SH} are increasing on average despite the challenges that models face when simulating their changes across different regions (Figure 2B). The global increase in *q* implies an increase in dew point temperatures used to calculate the heat index (i.e. the human perception of heat when incorporating humidity *sensu* Steadman (1979), see also Anderson et al., (2013)), which has also been increasing across the globe (Lee & Brenner, 2015) and is predicted to increase further (Dahl et al., 2019) which increases the likelihood of mortality, especially amongst vulnerable populations (Ahmadalipour & Moradkhani, 2018). It is notable that these changes in E_{SH} have contributed to significant increases in *E* across many subtropical and tropical areas (Fig. 1C) including major population centers in the Mediterranean and Middle East, South Asia, and East Asia, where atmospheric energy content is already in abundance and extreme heat index values have observed to be increasing (Lee & Brenner, 2015). As a consequence, had excess energy been partitioned to T_a, many of these tropical and subtropical regions would have seen T_a increases of nearly 3 °C across the 1980-2014 study period (Figure 3B) demonstrating the importance of E_{SH} to buffering T_a changes but noting also the importance of E_{SH} to human and animal comfort, often expressed using the cliche 'it's not the heat it's the humidity'. Both are important.

4.1 Conclusions

We argue that expressing global change in energy flux terms (Pielke et al., 2004, 2007) creates a richer understanding of changes to the Earth system from anthropogenic global change. From this perspective, ongoing efforts to compile and improve global humidity data products are critical for understanding recent climate changes (Willett et al., 2014, 2020). Focusing on T_a changes alone directs one's attention to the unprecedented changes of arctic regions (e.g. Figure 3A), and for good reason. Adding changes in E_{SH} due to *q* further emphasizes the importance of changes in *E* across the globe including tropical regions and major population centers (e.g. Figure 2C, 3B, and 4A). Focusing on extremes rather than means highlights the major changes that have occurred in subtropical areas further still; many of the largest changes in *E* have occurred in subtropical regions (Figure 4B). Despite our focus on the near-surface atmosphere, global changes to this small but important part of the earth system remain a small fraction of changes to the energy content of the Earth system due to global change (Church et al., 2011; Peterson et al., 2011; von Schuckmann et al., 2020). It is up to us to effectively communicate the magnitude of these changes to an often skeptical public (Moser, 2010), and we feel that emphasizing the unprecedented changes in atmospheric energy content is a logical way to do so.

Acknowledgments

We thank the AMIP model developers and MERRA-2 team for providing the data necessary to complete this study. PCS acknowledges support from the National Science Foundation Department of Environmental Biology grant #1552976 and the University of Wisconsin – Madison. We thank Gabriel Bromley, Anam Khan, Dr. Amy Trowbridge, Dr. Susanne Wiesner, and David Wood for valuable comments on earlier versions of this manuscript and students enrolled in LRES 464 and 465 at Montana State University for insight into how to communicate these concepts efficiently. No conflicts of interest are noted. Results of the present analyses are available on figshare at https://figshare.com/articles/dataset/Near_surface_energy_specific_humidity_and_temperature_changes_from_MERRA-2/13704796

References

Ahmadalipour, A., & Moradkhani, H. (2018). Escalating heat-stress mortality risk due to global warming in the Middle East and North Africa (MENA). *Environment International*, *117*, 215–225.

Anderson, G. B., Bell, M. L., & Peng, R. D. (2013). Methods to calculate the heat index as an exposure metric in environmental health research. *Environmental Health Perspectives*, *121*(10), 1111–1119.

Avissar, R. (1995). Recent advances in the representation of land-atmosphere interactions in general circulation models. *Reviews of Geophysics*. https://doi.org/10.1029/95rg00258

Bethke, I., Wang, Y., Counillon, F., Kimmritz, M., Fransner, F., Samuelsen, A., Langehaug, H. R., Chiu, P.-G., Bentsen, M., Guo, C., Tjiputra, J., Kirkevåg, A., Olivië, D. J. L., Seland, Ø., Fan, Y., Lawrence, P., Eldevik, T., Keenlyside, N. (2019). NCC NorCPM1 model output prepared for CMIP6 CMIP amip. Version 20191031.Earth System Grid Federation. https://doi.org/10.22033/ESGF/CMIP6.10863

Bosilovich, M. G., Robertson, F. R., Takacs, L., Molod, A., & Mocko, D. (2017). Atmospheric Water Balance and Variability in the MERRA-2 Reanalysis. *Journal of Climate*. https://doi.org/10.1175/jcli-d-16-0338.1

Boucher, O., Denvil, S., Caubel, A., Foujols, M. A. (2018). IPSL IPSL-CM6A-LR model output prepared for CMIP6 CMIP amip. Version 20191121.Earth System Grid Federation. https://doi.org/10.22033/ESGF/CMIP6.5113

Byrne, M. P., & O'Gorman, P. A. (2016). Understanding Decreases in Land Relative Humidity with Global Warming: Conceptual Model and GCM Simulations. *Journal of Climate*, *29*(24), 9045–9061.

Byun, Y.-H., Lim, Y.-J., Sung, H. M., Kim, J., Sun, M., Kim, B.-H. (2019). NIMS-KMA KACE1.0-G model output prepared for CMIP6 CMIP amip. Version 20190813. Earth

System Grid Federation. https://doi.org/10.22033/ESGF/CMIP6.8350

Chai, Z. (2020). CAS CAS-ESM1.0 model output prepared for CMIP6 CMIP amip. Version 20200303.Earth System Grid Federation. https://doi.org/10.22033/ESGF/CMIP6.3180

Cheng, L., Abraham, J., Trenberth, K. E., Fasullo, J., Boyer, T., Locarnini, R., et al. (2021). Upper Ocean Temperatures Hit Record High in 2020. *Advances in Atmospheric Sciences*. https://doi.org/10.1007/s00376-021-0447-x

Church, J. A., White, N. J., Konikow, L. F., Domingues, C. M., Graham Cogley, J., Rignot, E., et al. (2011). Revisiting the Earth's sea-level and energy budgets from 1961 to 2008. *Geophysical Research Letters*. https://doi.org/10.1029/2011gl048794

Dahl, K., Licker, R., Abatzoglou, J. T., & Declet-Barreto, J. (2019). Increased frequency of and population exposure to extreme heat index days in the United States during the 21st century. *Environmental Research Communications*, *1*(7), 075002.

Danabasoglu, G. (2019). NCAR CESM2 model output prepared for CMIP6 CMIP amip. Version 20200226.Earth System Grid Federation. https://doi.org/10.22033/ESGF/CMIP6.7522

Danabasoglu, G. (2020). NCAR CESM2-FV2 model output prepared for CMIP6 CMIP amip. Version 20200305.Earth System Grid Federation. https://doi.org/10.22033/ESGF/CMIP6.11287

Dessler, A. E., & Sherwood, S. C. (2009). Atmospheric science. A matter of humidity. *Science*, *323*(5917), 1020–1021.

Dix, M., Bi, D., Dobrohotoff, P., Fiedler, R., Harman, I., Law, R., Mackallah, C., Marsland, S., O'Farrell, S., Rashid, H., Srbinovsky, J., Sullivan, A., Trenham, C., Vohralik, P., Watterson, I., Williams, G., Woodhouse, M., Bodman, R., Dias, F. B., Domingues, C., Hannah, N., Heerdegen, A., Savita, A., Wales, S., Allen, C., Druken, K., Evans, B., Richards, C., Ridzwan, S., M., Roberts, D., Smillie, J., Snow, K., Ward, M., Yang, R. (2019). CSIRO-ARCCSS ACCESS-CM2 model output prepared for CMIP6 CMIP amip. Version 20191125.Earth System Grid Federation. https://doi.org/10.22033/ESGF/CMIP6.4239

Eyring, V., Bony, S., Meehl, G. A., Senior, C. A., Stevens, B., Stouffer, R. J., & Taylor, K. E. (2016). Overview of the Coupled Model Intercomparison Project Phase 6 (CMIP6) experimental design and organization. *Geoscientific Model Development*. https://doi.org/10.5194/gmd-9-1937-2016

Ficklin, D. L., & Novick, K. A. (2017). Historic and projected changes in vapor pressure deficit suggest a continental-scale drying of the United States atmosphere. *Journal of Geophysical Research: Atmospheres*. https://doi.org/10.1002/2016jd025855

Gelaro, R., McCarty, W., Suárez, M. J., Todling, R., Molod, A., Takacs, L., et al. (2017). The Modern-Era Retrospective Analysis for Research and Applications, Version 2 (MERRA-2). *Journal of Climate*, *30*(Iss 13), 5419–5454.

Held, I. M., & Soden, B. J. (2006). Robust Responses of the Hydrological Cycle to Global Warming. *Journal of Climate*. https://doi.org/10.1175/jcli3990.1

Held, I. M., Delworth, T. L., Lu, J., Findell, K. L., & Knutson, T. R. (2005). Simulation of Sahel drought in the 20th and 21st centuries. *Proceedings of the National Academy of Sciences of the United States of America*, *102*(50), 17891–17896.

Kostov, Y., Ferreira, D., Armour, K. C., & Marshall, J. (2018). Contributions of greenhouse gas forcing and the southern annular mode to historical southern ocean surface temperature trends. *Geophysical Research Letters*, *45*(2), 1086–1097.

Lee, D., & Brenner, T. (2015). Perceived temperature in the course of climate change: an analysis of global heat index from 1979 to 2013. *Earth System Science Data*, *7*(2), 193–202.

Ligges, U., Short, T., Kienzle, P., Schnackenberg, S., Billinghurst, D., Borchers, H. W., & Weingessel, A. (2013). signal: Signal processing. R Package Version 0.7-3.

McVicar, T. R., Roderick, M. L., Donohue, R. J., Li, L. T., Van Niel, T. G., Thomas, A., et al. (2012). Global review and synthesis of trends in observed terrestrial near-surface wind speeds: Implications for evaporation. *Journal of Hydrology*. https://doi.org/10.1016/j.jhydrol.2011.10.024

Moser, S. C. (2010). Communicating climate change: history, challenges, process and future directions: Communicating climate change. *Wiley Interdisciplinary Reviews. Climate Change*, *1*(1), 31–53.

NASA Goddard Institute for Space Studies (NASA/GISS) (2018). NASA-GISS GISS-E2.1G model output prepared for CMIP6 CMIP amip. Version 20190910.Earth System Grid Federation. https://doi.org/10.22033/ESGF/CMIP6.6984

Park, S., Shin, J. (2019). SNU SAM0-UNICON model output prepared for CMIP6 CMIP amip. Version 20190323.Earth System Grid Federation. https://doi.org/10.22033/ESGF/CMIP6.7784

Peterson, T. C., Willett, K. M., & Thorne, P. W. (2011). Observed changes in surface atmospheric energy over land. *Geophysical Research Letters*. https://doi.org/10.1029/2011gl048442

Pielke, R. A., Davey, C., & Morgan, J. (2004). Assessing “global warming” with surface heat content. *Eos, Transactions American Geophysical Union*. https://doi.org/10.1029/2004eo210004

Pielke, R. A., Davey, C. A., Niyogi, D., Fall, S., Steinweg-Woods, J., Hubbard, K., et al. (2007).

Unresolved issues with the assessment of multidecadal global land surface temperature trends. *Journal of Geophysical Research*. https://doi.org/10.1029/2006jd008229

Pohlert, T. (2020). trend: Non-Parametric Trend Tests and Change-Point Detection. R package version 1.1.4. https://CRAN.R-project.org/package=trend.

R Core Team (2020). R: A Language and Environment for Statistical Computing. R Foundation for Statistical Computing. https://www.R-project.org/.

Reid, P. C., Hari, R. E., Beaugrand, G., Livingstone, D. M., Marty, C., Straile, D., et al. (2016). Global impacts of the 1980s regime shift. *Global Change Biology*, *22*(2), 682–703.

Ridley, J., Menary, M., Kuhlbrodt, T., Andrews, M., Andrews, T. (2019). MOHC HadGEM3-GC31-LL model output prepared for CMIP6 CMIP amip. Version 20191001.Earth System Grid Federation. https://doi.org/10.22033/ESGF/CMIP6.5853

Rye, C. D., Marshall, J., Kelley, M., Russell, G., Nazarenko, L. S., Kostov, Y., et al. (2020). Antarctic glacial melt as a driver of recent southern ocean climate trends. *Geophysical Research Letters*, *47*(11), e2019GL086892.

Schneider, T., O'Gorman, P. A., & Levine, X. J. (2010). Water vapor and the dynamics of climate changes. *Reviews of Geophysics* , *48*(3). https://doi.org/10.1029/2009rg000302

Tatebe, H., Watanabe, M. (2018). MIROC MIROC6 model output prepared for CMIP6 CMIP amip. Version 20181214.Earth System Grid Federation. https://doi.org/10.22033/ESGF/CMIP6.5422

von Schuckmann, K., Cheng, L., Palmer, M. D., Tassone, C., Aich, V., Adusumilli, S., et al. (2020). Heat stored in the Earth system: Where does the energy go? The GCOS Earth heat inventory team. *Earth System Science Data*, *12*, 2013–2041.

Schwartz, S. E., & Andreae, M. O. (1996). Uncertainty in Climate Change Caused by Aerosols.

Science. https://doi.org/10.1126/science.272.5265.1121

Steadman, R. G. (1979). The Assessment of Sultriness. Part I: A Temperature-Humidity Index Based on Human Physiology and Clothing Science. *Journal of Applied Meteorology and Climatology*, *18*(7), 861–873.

Stroeve, J., Holland, M. M., Meier, W., Scambos, T., & Serreze, M. (2007). Arctic sea ice decline: Faster than forecast. *Geophysical Research Letters*, *34*(9). Retrieved from https://agupubs.onlinelibrary.wiley.com/doi/abs/10.1029/2007GL029703@10.1002/(ISSN)1944-8007.GRL40

Voldoire, A. (2019). CNRM-CERFACS CNRM-CM6-1 model output prepared for CMIP6 GMMIP amip-hist. Version 20190711.Earth System Grid Federation. https://doi.org/10.22033/ESGF/CMIP6.3931

Willett, K. M., Dunn, R. J. H., Thorne, P. W., Bell, S., de Podesta, M., Parker, D. E., et al. (2014). HadISDH land surface multi-variable humidity and temperature record for climate monitoring. *Climate of the Past*, *10*(6), 1983–2006.

Willett, K. M., Dunn, R. J. H., Kennedy, J. J., & Berry, D. I. (2020). Development of the HadISDH.marine humidity climate monitoring dataset. *Earth System Science Data*. https://doi.org/10.5194/essd-12-2853-2020

Xiang, B., Blanton, C., Guo, H., Harris, L., Held, I. M., John, J. G., McHugh, C., Ming, Y., Ploshay, J., Radhakrishnan, A., Rand, K., Vahlenkamp, H., Wilson, C., Zhao, M. (2018). NOAA-GFDL GFDL-CM4 model output prepared for CMIP6 GMMIP amip-hist. Version 20180701. Earth System Grid Federation. https://doi.org/10.22033/ESGF/CMIP6.8504

Yukimoto, S., Koshiro, T., Kawai, H., Oshima, N., Yoshida, K., Urakawa, S., Tsujino, H., Deushi, M., Tanaka, T., Hosaka, M., Yoshimura, H., Shindo, E., Mizuta, R., Ishii, M., Obata, A., Adachi, Y. (2019). MRI MRI-ESM2.0 model output prepared for CMIP6 GMMIP amip-hist. Version 20200120.Earth System Grid Federation. https://doi.org/10.22033/ESGF/CMIP6.6764

Zeng, N., Neelin, J. D., Lau, K., & Tucker, C. J. (1999). Enhancement of Interdecadal Climate Variability in the Sahel by Vegetation Interaction. *Science*, *286*(5444), 1537–1540.

Ziehn, T., Chamberlain, M., Lenton, A., Law, R., Bodman, R., Dix, M., Wang, Y., Dobrohotoff, P., Srbinovsky, J., Stevens, L., Vohralik, P., Mackallah, C., Sullivan, A., O'Farrell, S., Druken, K. (2019). CSIRO ACCESS-ESM1.5 model output prepared for CMIP6 CMIP amip. Version 20191205.Earth System Grid Federation. https://doi.org/10.22033/ESGF/CMIP6.4240

Tables

Table 1: Models prepared for the Atmospheric Model Intercomparison Project (Eyring et al., 2016) that included near-surface temperature and specific humidity products used in the present analysis. Models have a resolution of 100 km except those with stars indicate 250 km resolution.

Model	Reference
CAS-ESM 1.0	Chai (2020)
CNRM-CM6-1*	Voldoire (2019)
CSIRO-ARC*	Dix et al. (2019)
ACCESS-ESM1.5*	Ziehn et al. (2019)
IPSL-CM6A-LR*	Boucher et al. (2018)
MIROC6*	Tatebe et al. (2018)
HadGEM3-GC31-LL*	Ridley et al. (2019)
MRI-ESM2.0	Yukimoto et al. (2019)
GISS-E2.1G*	NASA Goddard Institute for Space Studies (2018)
CESM2	Danabasoglu (2019)
CESM2-FV2*	Danabasoglu (2020)
NCC NorCPM1*	Bethke et al. (2019)
NIMS-KMA KACE1.0-G*	Byun et al. (2019)
GFDL-CM4	Xiang et al. (2018)
SAM0-UNICON	Park et al. (2019)